INTRODUCTION TO RF LINEAR ACCELERATORS

N. Pichoff
CEA/DIF/DPTA/SP2A/LFPA, France

Abstract
After a short introduction to applications of RF linacs and their advantages and drawbacks as opposed to circular accelerators, the model of RF resonant cavities and their excitation by RF sources or beam is introduced. Then beam dynamics notions, essential to linacs, such as transit-time factor, synchronism, r.m.s. properties, matching and mismatching in linear or non-linear forces, are presented.

1 INTRODUCTION

A one-hour lecture on RF linear accelerators (linacs) and a ten-hour course were given to the CAS students. The short lecture introduced the students to RF specifics and beam dynamics basics giving them a good understanding of linacs. This paper deals with the notions introduced in the lecture. Students eager to learn more about linacs are advised to read the books in Refs. [1] and [2].

After a short introduction to RF linac applications and their advantages/disadvantages as opposed to circular accelerators, this paper is divided into two parts:

– Section 3 introduces the RF cavity through its basic principle and model, the notion of RF modes, and the way they are excited either from the RF source or by the beam.

– Section 4 gives useful notions of beam dynamics in linacs: the transit time factor; the notion of synchronism; the particle motion in continuous non-linear forces (longitudinal dynamics); and periodic linear forces (transverse dynamics). The notion of beam r.m.s. properties and matching in the linac is discussed. The effects of non-linear forces on emittance growth are introduced.

2 WHY RF LINACS?

The goal of a particle accelerator is to produce a '*low-cost wanted*' beam. By '*wanted*', one means a given particle type, with a given intensity, at a given energy within a given emittance (or brightness) in a given time structure. Costs should cover construction, operation, and personnel.

Synchrotrons, cyclotrons, and RF linear accelerators (linacs)[1] can all achieve this.

The main advantages of linacs are that

– they can handle high current beams (they are less limited by tune shift),

– they can run in high duty-cycle (the beam passes only once at each position),

– they exhibit low synchrotron radiation losses (no dipoles).

Their main drawbacks are that

– they consume space and cavities,

– the synchrotron radiation damping of light particles (electrons/positrons) cannot be easily used to reduce the beam emittance.

[1] Electrostatic machines are also suitable for low-current, low-energy beams.

That is why linacs are mainly used:

– as low-energy injectors (where the space-charge force is more important and the duty-cycle is high),

– with high-intensity/power proton beams (high space-charge level or/and duty cycle),

– in new lepton collider projects at very high energy (no radiation losses).

3 RF CAVITIES

The RF cavity gives energy to the beam. As the cost of the RF generally represents the main expense of the linac structure apart from the building, the choice of the RF structure has to be studied very carefully. This paper presents only the principle of an RF cavity. More precise information can be found in the CAS dedicated to RF [3].

3.1 A standing-wave RF cavity

3.1.1 Field calculation

An RF cavity is simply a piece of conductor enclosing an empty volume (generally a vacuum). Solutions of Maxwell's equations in this volume, taking into account the boundary conditions on the conductor, allow the existence of electromagnetic field configurations in the cavity. These are called the *resonant modes*.

Maxwell's equations

$$\vec{\nabla}\cdot\vec{E}=\frac{\rho}{\varepsilon_0}, \qquad \vec{\nabla}\cdot\vec{B}=0,$$

$$\vec{\nabla}\times\vec{E}=-\frac{\partial\vec{B}}{\partial t}, \qquad \vec{\nabla}\times\vec{B}=\mu_0\vec{J}+\frac{1}{c^2}\cdot\frac{\partial\vec{E}}{\partial t}.$$

$\mu_0 = 4\pi\cdot10^{-7}$ T·m·A^{-1} : permeability of free space,
$\varepsilon_0 = 1/\mu_0 c^2$: permittivity of free space,
$c = 2.99792458\cdot10^{8}$ m·s^{-1} : speed of light in vacuum.

Boundary conditions

$$\vec{n}\times\vec{E}_n=\vec{0}, \qquad \vec{n}\cdot\vec{B}_n=\vec{0},$$

$$\vec{n}\cdot\vec{E}_n=\frac{\Sigma}{\varepsilon_0}, \qquad \vec{n}\times\vec{H}_n=\vec{K}.$$

$\vec{n}$, the normal to the conductor,
Σ (C/m^2), the surface charge density,
$\vec{K}$ (A/m), the surface current density.

Each mode, labelled *n*, is characterized by an electromagnetic field amplitude configuration $\vec{E}_n(\vec{r})/\vec{B}_n(\vec{r})$ oscillating with an RF frequency f_n. The electric field amplitude configuration is the solution of the equation:

$$\vec{\nabla}^2\vec{E}_n+\frac{\omega_n^2}{c^2}\cdot\vec{E}_n=\vec{0}, \tag{1}$$

where $\vec{E}_n(\vec{r})$ should satisfy the boundary conditions and $\omega_n=2\pi\cdot f_n$ is the mode pulsation.

The electric field in the cavity is a weighted sum of all the modes:

$$\vec{E}(\vec{r},t)=\sum e_n(t)\cdot\vec{E}_n(\vec{r})=\sum a_n\cdot e^{j\omega_n t}\cdot\vec{E}_n(\vec{r}) \ . \tag{2}$$

Here a_n is a complex number and $e_n(t)$ is the field variation with time, it is the solution of [4]:

$$\ddot{e}_n + \omega_n^2 \cdot e_n = -\frac{\omega_n^2}{\sqrt{\varepsilon\mu}} \cdot \int_S \left(\vec{E} \times \vec{H}_n\right) \cdot \vec{n} \cdot dS + \frac{1}{\varepsilon}\frac{d}{dt}\int_{S'} \left(\vec{H} \times \vec{E}_n\right) \cdot \vec{n} \cdot dS' - \frac{1}{\varepsilon}\frac{d}{dt}\int_V \vec{J}(\vec{r},t) \cdot \vec{E}_n(\vec{r}) \cdot dV \quad . \tag{3}$$

Here $\vec{H}$ is the magnetic induction. It is often used close to the surface in place of $\vec{B}$, as unlike $\vec{B}$, it is macroscopically continuous through the surface. $\vec{J}$ is the current density, of the beam for example. The first term on the right-hand side is an integration over the conductor which is not a perfect conductor. Because of power losses by Joule effects, it can be rewritten as a damping term:

$$-\frac{\omega_n}{Q_{0n}} \cdot \dot{e}_n \,. \tag{4}$$

The calculation of Q_{0n}, the *quality factor of the mode*, can be deduced from power loss considerations:

$U_n(0)$ is the energy stored by the n-mode at time $t = 0$. For $t > 0$, no more power is injected in the cavity. Let us define $k(t)$ as:

$$k(t) = \frac{e_n(t)}{e_n(t=0)} \,. \tag{5}$$

The energy lost per unit time is the power dissipated in the conductor P_n:

$$\frac{dU_n(t)}{dt} = -P_n(t) \,. \tag{6}$$

The average power dissipated in the conductor per cycle is proportional to the square of the current density (and then the magnetic field) close to the surface:

$$P_n = \frac{R_s}{2}\int_S K_n^2 dS = \frac{R_s}{2}\int_S H_n^2 dS \,, \tag{7}$$

where R_s is the *surface resistance* defined as:

$$-R_s = \sqrt{\frac{\mu_0 \pi f_0}{\sigma}} \,, \text{ for } \textit{normal conductors} \tag{8}$$

where σ is the conductor conductivity ($1/\sigma = 1.7 \cdot 10^{-7}$ Ω·m for copper).

$$-R_s \approx R_{res} + 9 \cdot 10^{-5} \frac{f_0^2\,(\mathrm{GHz})}{T\,(\mathrm{K})} \exp\left(-1.92 \cdot \frac{T_c}{T}\right), \text{ for } \textit{superconducting niobium} \tag{9}$$

where R_{res} is the residual resistance (10^{-9}–10^{-8} Ω) depending on the surface imperfections, T is the working absolute temperature, $T_c = 9.2$ K is the critical temperature.

From Eqs. (5) and (7) can be deduced:

$$P_n(t) = k(t)^2 \cdot P_n(t=0) \,. \tag{10}$$

The stored energy is proportional to the square of the field:

$$U_i = \frac{\varepsilon_0}{2}\iiint \left\|\vec{E}_i\right\|^2 dv = \frac{1}{2\mu_0}\iiint \left\|\vec{B}_i\right\|^2 dv \,, \tag{11}$$

then:

$$U_n(t) = k(t)^2 \cdot U_n(t=0) \,. \tag{12}$$

Equation (6) becomes:

$$\frac{dk^2}{dt} = -\frac{P_n}{U_n} \cdot k^2 = 2 \cdot k\dot{k}\,, \tag{13}$$

giving :

$$\frac{de_n}{dt} = -\frac{P_n}{2 \cdot U_n} \cdot e_n\,. \tag{14}$$

A comparison with the damping term written in (4) gives:

$$\boxed{Q_{0n} = \frac{\omega_n \cdot U_n}{P_n}}\ . \tag{15}$$

In the second term, the integration is performed over the open surfaces S' and represents the coupling with the outside system. This coupling can be divided into two contributions:

- the injected power coming from the power generator through the coupler,
- an additional damping, which can be represented by another quality factor Q_{exn} known as the *external Q*, corresponding to power losses through the opened surfaces. The coupling can be calculated from the coupler geometry with electromagnetic codes.

$$-\frac{\omega_n}{Q_{\text{exn}}} \cdot \dot{e}_n + S_n \cdot e^{j(\omega_{\text{RF}} t + \varphi_0)}\ . \tag{16}$$

$S_n \cdot e^{j(\omega_{\text{RF}} t + \varphi_0)}$ is the RF source filling through the coupler.

The last term, represents the field excited by the beam, known as the beam loading. It is proportional to the beam intensity:

$$k_n \cdot I(t)\ . \tag{17}$$

$I(t)$ is a complex number (it has a phase) representing the beam current.

Equation (3) can then be modelized by:

$$\boxed{\frac{d^2 e_n}{dt^2} + \frac{\omega_{\text{RF}}}{Q_n} \cdot \frac{de_n}{dt} + \omega_n^2 \cdot e_n = S_n \cdot e^{j(\omega_{\text{RF}} t + \varphi_0)} + k_n \cdot I(t)}\ , \tag{18}$$

which is the equation of a damped harmonic oscillator in a forced regime. Q_n is the quality factor of the cavity, with

$$\frac{1}{Q_n} = \frac{1}{Q_{0n}} + \frac{1}{Q_{\text{exn}}},$$

and

$$\tau = 2 \cdot \frac{Q_n}{\omega_{\text{RF}}}$$

is the cavity filling time.

Note that both the coupler or the beam can excite some RF modes.

Equation (18) shows an RLC circuit which is often used to modelize the system. A complete study of this model can be found in Ref. [4].

From these modes, one with a field amplitude along the longitudinal direction on the axis is used to accelerate the beam. The geometry of the cavity is then calculated to match the frequency of this accelerating mode to the RF frequency. This mode is excited in the cavity through a power coupler whose geometry is calculated and adjusted to transfer electromagnetic energy in the cavity to the beam without reflection—a process called coupler matching.

3.1.2 Shunt impedances

To first order, only the accelerating mode is excited in the cavity. The transverse component of the electric field is generally null along the axis. An expression of the *z* component of the field on the axis is then:

$$E_z(s,t) = E_{z0}(s) \cdot \cos(\omega t + \varphi). \tag{19}$$

The field amplitude is $E_{z0}(s)$.

One defines the *cavity voltage* V_0 as:

$$V_0 = \int_{-\infty}^{+\infty} |E_{z0}(s)| \cdot ds. \tag{20}$$

Then $q \cdot V_0$ represents the maximum energy (in eV) that a particle with charge q could gain if the field was always maximum.

Let P_d be the *power deposition in the cavity*:

$$P_d = \frac{V_0^2}{2 \cdot R}. \tag{21}$$

The *cavity shunt impedance R* is very useful in cavity design. For optimum acceleration, it has to be as high as possible.

Because the electric field changes with time as the particle transits through the cavity, the maximum energy $q \cdot V$ that can be gained in the cavity by a particle of charge q is lower than $q \cdot V_0$. One defines the *transit-time factor T* as:

$$T = \frac{V}{V_0} \leq 1. \tag{22}$$

This corrective factor to the energy gain takes the particle transit time in the cavity into account, and is obviously dependent on the particle velocity. The calculation of this factor is described in Section 4.

The *effective shunt impedance* RT^2 is then proportional to the ratio between the square of the maximum energy ΔU_{max} that can be gained by the beam and the power lost in the cavity:

$$RT^2 = \frac{\Delta U_{max}^2}{2P_d}. \tag{23}$$

It is some sort of cavity efficiency and has to be maximum.

The shunt impedance is often used to compare the efficiency of different structures at a given energy. Usually, the geometry is different, so one extends the preceding definition per unit length to allow a better comparison.

Let L be the cavity length[2]. The mean cavity electric field E_0 is defined as:

$$E_0 = \frac{V_0}{L}. \tag{24}$$

The power deposition per unit length in the cavity P_d' is then:

$$P_d' = \frac{E_0^2}{2 \cdot Z}, \tag{25}$$

where Z is the *cavity shunt impedance per unit length.*

The *effective shunt impedance per unit length* ZT^2 is then proportional to the ratio between the square of the maximum energy $\Delta U'_{max}$ that can be gained per unit length by the beam and the power lost per unit length in the cavity:

$$ZT^2 = \frac{\Delta U'^2_{max}}{2P'_d}. \tag{26}$$

As it is depending on the particle velocity, one chooses the structure that maximize ZT^2 at a given energy. Figure 1 represents the evolution of the effective shunt impedance per metre for two different structures (SDTL and CCL) with different apertures ϕ. The higher the aperture (space for beam), the lower the effective shunt impedance. SDTL structures are more efficient at lower energy, CCL structures are more efficient at higher energy. The optimum transition energy is around 100 MeV for protons.

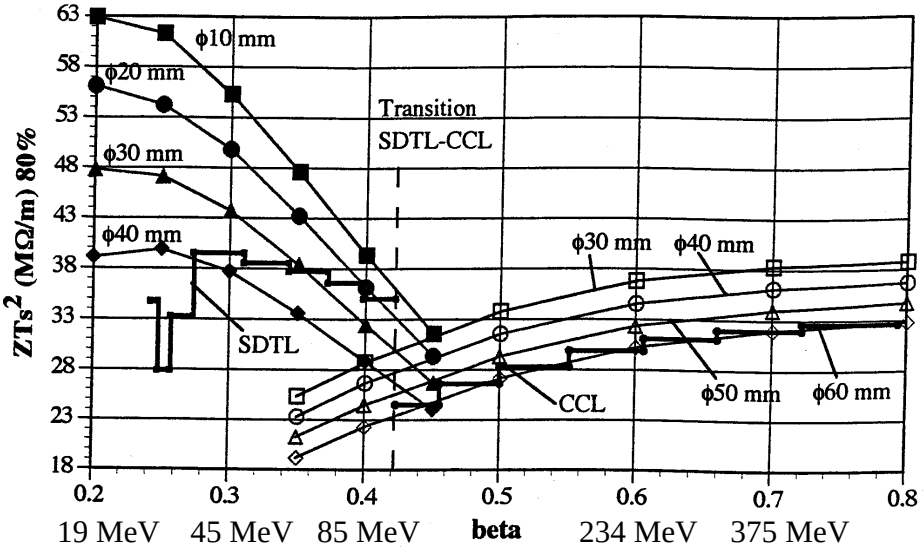

Fig. 1: Effective shunt impedance per metre of different TRISPAL structures (C. Bourat)

3.2 A travelling-wave RF cavity

A travelling-wave cavity is generally used to accelerate ultrarelativistic particles. These cavities generally have two power ports. One where the power enters, and another, at the other end, where the power exits (Fig. 2). The electric field travels through the cavity from the input to the output port. Its phase velocity is adjusted to the beam velocity. The field phase is adjusted to continuously accelerate the beam.

[2] Owing to the cavity fringe field, L is often arbitrarily defined as the physical length of the cavity.

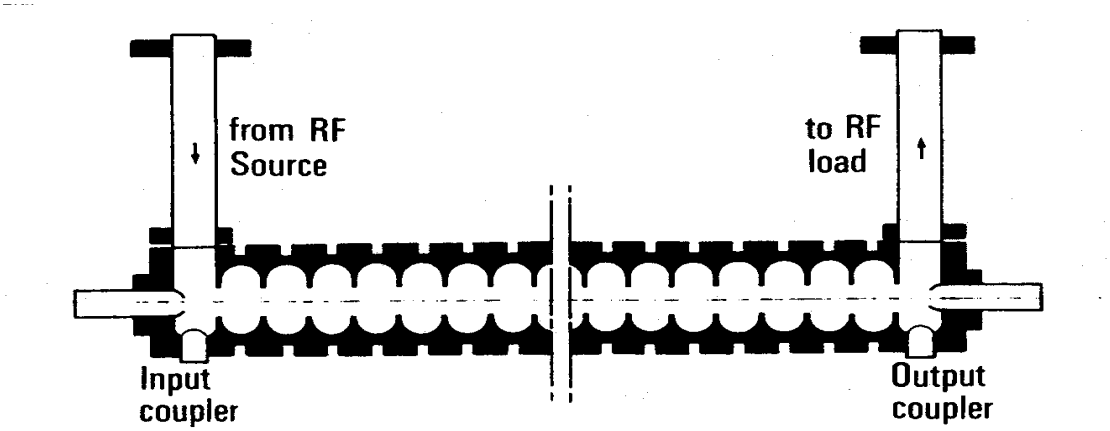

Fig. 2: A travelling-wave cavity

The RF phase velocity in empty cavities or wave-guides is usually higher than (or equal to) the speed of light in vacuum *c*. As particle velocity cannot exceed *c*, the RF phase velocity should be decelerated to reach the synchronism condition by introducing some periodic obstacles into the guide (such as iris-loaded waveguide). The periodic field can then be expanded into a Fourier series with different wave numbers:

$$Ez(t,z) = \sum_{n=-\infty}^{+\infty} ez_n \cdot \exp\left[j \cdot (\omega t - k_n z) \right] , \tag{27}$$

with ez_n the *space harmonic* amplitude, k_n the space harmonic wave numbers,

$$k_n = k_0 + \frac{2\pi n}{d} \quad , \tag{28}$$

d the obstacle period, and k_0 the waveguide number.

The phase velocity v_n of space harmonic number n is

$$v_n = \frac{\omega}{k_n} . \tag{29}$$

Particles whose velocity is close to the phase velocity of one space harmonic exchange energy with it. Otherwise, the average effect is null.

A complete calculation of these insertion obstacles as well as a large bibliography can be found in Ref. [5]. This kind of travelling-wave accelerating structure is mainly used to accelerate ultra-relativistic electrons.

Moreover, the model of a travelling-wave acceleration, even with acceleration with standing-wave cavities, is often used to simplify the calculation of the longitudinal-motion equations.

4 ELEMENTS OF BEAM DYNAMICS

4.1 The transit-time factor and the particle synchronous phase

A cavity has a finite length L. The cavity input abscissa is s_0, and $E_z(s)$ is the amplitude of the electric field longitudinal component on axis.

The energy[3] gained by a charged particle on axis in the cavity is

[3] This is actually the longitudinal energy, but we can consider that there is no transverse field on the cavity axis.

$$\Delta W = \int_{s_0}^{s_0+L} qE_z(s)\cdot\cos\left[\phi(s)\right]\cdot ds \ , \tag{30}$$

where q is the particle charge, $\phi(s)$ is the cavity RF phase when the particle is at abscissa s. It is defined as

$$\phi(s) = \phi_0 + \frac{\omega}{c}\int_{s_0}^{s_0+s}\frac{ds'}{\beta_z(s')} \ , \tag{31}$$

where $\phi_0 = \phi(s_0)$ is the RF phase when the particle enters the cavity.

Writing $\phi(s) = \phi(s) + (\phi_s - \phi_s)$, ϕ_s being an arbitrary phase and using trigonometric relationships, one gets for the energy gain:

$$\Delta W = \cos\phi_s\cdot\int_{s_0}^{s_0+L} qEz(s)\cdot\cos\left[\phi(s)-\phi_s\right]\cdot ds - \sin\phi_s\cdot\int_{s_0}^{s_0+L} qEz(s)\cdot\sin\left[\phi(s)-\phi_s\right]\cdot ds \ . \tag{32}$$

By defining ϕ_s as:

$$\int_{s_0}^{s_0+L} qEz(s)\cdot\sin\left[\phi(s)-\phi_s\right]\cdot ds = 0 \ ,$$

giving the definition of the *synchronous phase* ϕ_s:

$$\boxed{\phi_s = \arctan\left(\frac{\displaystyle\int_{s_0}^{s_0+L} Ez(s)\cdot\sin\left[\phi(s)\right]\cdot ds}{\displaystyle\int_{s_0}^{s_0+L} Ez(s)\cdot\cos\left[\phi(s)\right]\cdot ds}\right)} \ , \tag{33}$$

one finally gets

$$\boxed{\Delta W = \left(q\int_{s_0}^{s_0+L}\left|Ez(s)\right|\cdot ds\right)\cdot T\cdot\cos\phi_s = qV_0\cdot T\cdot\cos\phi_s} \ , \tag{34}$$

with

$$\boxed{T = \frac{1}{V_0}\int_{s_0}^{s_0+L} Ez(s)\cdot\cos\left[\phi(s)-\phi_s\right]\cdot ds} \ . \tag{35}$$

The *transit-time factor* T, depends on the particle initial velocity as well as on the field amplitude. This definition does not make any assumption about the field shape (no symmetry) resulting from a slightly different synchronous-phase definition, which can be found in the literature (which is often taken as the RF phase when the particle reaches mid-cavity). When the velocity gain in the cavity is much lower than the input-particle velocity, T depends only on the velocity and can be easily tabulated.

The calculation of T with formula (35) is sometimes difficult to perform, as ϕ_s has to be known. In fact, T does not depend on ϕ_s when the velocity gain is small and another formula (a little bit more difficult to understand physically) can be used:

$$\boxed{T = \frac{1}{V_0}\left|\int Ez(s)\cdot e^{j\phi(s)}\cdot ds\right|} \quad . \tag{36}$$

4.2 Notion of synchronism

A linac is designed so that one theoretical particle called the *synchronous particle* enters successively along the axis of RF cavities with a wanted RF phase law in order to get a wanted energy gain. This very important notion of synchronism allows the understanding of the efficiency and the stability of linacs.

Particles can be accelerated with travelling waves as well as standing waves (Fig. 3).

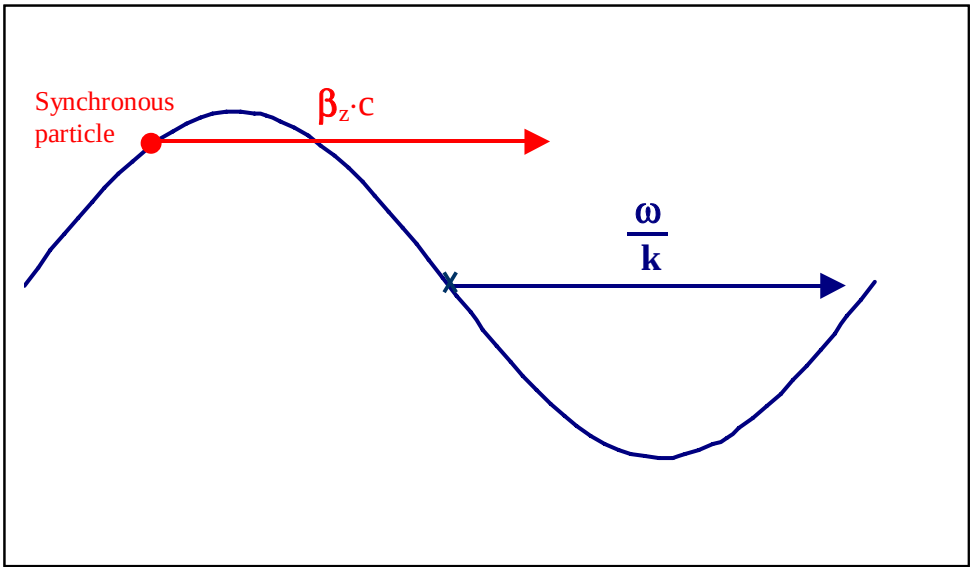

Fig. 3: Particle accelerated by a travelling wave

4.2.1 Acceleration with travelling waves

The on-axis RF accelerating field can be written as:

$$E_z(z,t) = E_0\cdot\cos(\omega t - kz), \tag{37}$$

where ω is the RF pulsation and k is the RF wave number.

The synchronism condition is reached when the particle-longitudinal velocity equals the RF phase velocity:

$$\beta_z\, c = \frac{k}{\omega}. \tag{38}$$

Here c is the speed of light in vacuum, β_z is the reduced longitudinal velocity of the synchronous particle. Note that when the *paraxial approximation*[4] is used, β_z is replaced by β, the reduced total speed of the particle.

[4] As $\beta = \beta_z\cdot\sqrt{1+x'^2+y'^2}$, paraxial approximation occurs when $x' << 1$ and $y' << 1$.

4.2.2 Standing waves

In most linacs, the beam is accelerated with RF cavities or gaps operating in standing-wave conditions. An RF power, produced by one or many RF sources, is introduced through a coupler in a resonant cavity exciting the wanted standing-wave accelerating mode. The cavity shape has been calculated and adjusted to match the accelerating mode to the power-supply frequencies and to throw the other mode frequencies far from the RF one.

As a first step, let us assume a set of thin independently phased RF cavities along the beam path (Fig. 4).

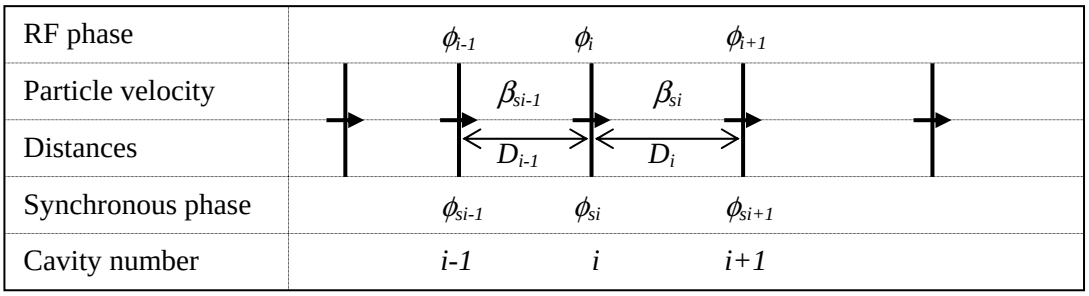

Fig. 4: A set of independently phased cavities

– ϕ_i is the absolute RF phase in the i^{th} cavity when $t = 0$ (the $t = 0$ instant has been arbitrarily chosen),

– β_{si} is the synchronous, particle reduced velocity at the i^{th} cavity output,

– ϕ_{si} is the RF synchronous phase of the i^{th} cavity of the synchronous particle[5],

– D_i is the distance between the i^{th} and the i+1th cavities.

The synchronism condition is reached when:

$$\phi_{si+1} - \phi_{si} = 2\pi \cdot \frac{D_i}{\beta_{s\,i}\lambda} + \phi_{i+1} - \phi_i + [2\pi n]. \tag{39}$$

The RF wavelength is $\lambda = c / f$.

One observes that the synchronism condition does not depend on the RF field amplitude. It has a non-intuitive consequence: an increase of the accelerating field amplitude in the cavities without phase change does not induce an increase of the synchronous-particle final energy but a change of the synchronous phase fulfilling the synchronism condition.

Two different kinds of structures exist:

– The coupled-cavity structures where the phase between cavities is fixed. The synchronism condition is achieved by adjusting the distance between the cavities.

In a Drift-Tube Linac (DTL), for example, the phase difference between the cells is fixed (= 2π). The distance between cells is then calculated to have:

$$D_i = \left(\frac{\phi_{si+1} - \phi_{si}}{2\pi} + 1 \right) \cdot \beta_{s\,i}\lambda \ . \tag{40}$$

[5] Do not confuse the *synchronous-particle phase*, the phase of the synchronous particle in a cavity and a *particle synchronous-phase*, the synchronous phase of a particle (whatever it is) in a cavity.

– The independent cavity structures where the distance between cavities is fixed. The synchronism condition is then achieved by adjusting the phase difference between the cavities.

In a Superconducting-Cavity Linac (SCL), for example, the distance between cavities is fixed by the cryogenics mechanism. The phase difference between cavities is then calculated to have:

$$\phi_{i+1} - \phi_i = \phi_{si+1} - \phi_{si} - 2\pi \cdot \frac{D_i}{\beta_{s\,i}\lambda} + [2\pi n]. \tag{41}$$

4.3 Particle motion in electromagnetic fields

4.3.1 Basis

The electromagnetic field can be divided into two contributions:

– The electric field: $\vec{E}$.

– The magnetic field: $\vec{B}$.

The intensity of these contributions depends on the referential where they are expressed. The equation of motion of a particle of charge q in these fields is:

$$\frac{d\vec{p}}{dt} = q \cdot \left(\vec{v} \times \vec{B} + \vec{E}\right), \tag{42}$$

where $\vec{p}$ is the momentum of the particle and $\vec{v}$ is its velocity.

Let us call s the abscissa of the beam in the linac path (rather than z to avoid any confusion with the particle longitudinal position in the bunch), the equation of motion can be rewritten:

$$\frac{d\vec{p}}{ds} = q \cdot \frac{\vec{v} \times \vec{B} + \vec{E}}{v_z}, \tag{43}$$

where v_z is the particle longitudinal velocity.

A projection on the Cartesian axis[6] (x, y, z) gives:

$$\boxed{\begin{cases} \dfrac{d\gamma\beta_x}{ds} = \dfrac{q}{mc} \cdot \left(y'B_z - B_y + \dfrac{E_x}{v_z} \right) = \dfrac{d\gamma\beta_z x'}{ds} \\ \dfrac{d\gamma\beta_y}{ds} = \dfrac{q}{mc} \cdot \left(B_x - x'B_y + \dfrac{E_y}{v_z} \right) = \dfrac{d\gamma\beta_z y'}{ds} \\ \dfrac{d\gamma\beta_z}{ds} = \dfrac{q}{mc} \cdot \left(x'B_y - y'B_x + \dfrac{E_z}{v_z} \right) \end{cases}}. \tag{44}$$

Here

$$x' = \frac{dx}{ds} = \frac{p_x}{p_z} = \frac{\beta_x}{\beta_z}$$

and

$$y' = \frac{dy}{ds} = \frac{p_y}{p_z} = \frac{\beta_y}{\beta_z}$$

[6] In general, x and y play the same role in a linac (contrary to their role in a circular accelerator).

are the slopes of the particle, and

$$\beta_w = \frac{v_w}{c},$$

is the reduced velocity *w*-component, *w* being *x*, *y* or *z*; v_w is the particle velocity *w* component; *m* and *q* are, respectively, the rest mass and the particle charge; *c* is the speed of light.

One clearly observes that longitudinal and transverse motions are coupled. However, for an easier understanding, and because the coupling is often very weak, the longitudinal and the transverse motions are usually treated as uncoupled, the longitudinal velocity v_z variations are considered separately. To uncouple the transverse and longitudinal motions, the *paraxial approximation* has to be done.

4.3.2 Paraxial approximation

The *paraxial approximation* is based on the assumption that $x'^2 + y'^2 << 1$.

Its natural consequence is

$$\beta_z = \beta \cdot \sqrt{1 + x'^2 + y'^2} \approx \beta . \tag{45}$$

For x' < 100 mrad and y' < 100 mrad, the error on β (or β_z) is lower than 1% .

This approximation is quite accurate at high energy where the beam divergence is small, but is more difficult to justify at very low energy.

4.3.3 Energy gain calculation

From Eqs. (44), one can easily obtain the energy gain:

$$\frac{d\gamma}{ds} = \beta_z \left(x' \cdot \frac{d\gamma\beta_x}{ds} + y' \cdot \frac{d\gamma\beta_y}{ds} + \frac{d\gamma\beta_x}{ds} \right) , \tag{46}$$

giving:

$$\boxed{\frac{d\gamma}{ds} = \frac{q}{mc^2} \cdot \left(x'E_x + y'E_y + E_z \right)} . \tag{47}$$

One finds the well-known result that only the electric field contributes to energy gain.

4.4 Longitudinal particle dynamics (motion in non-linear force)

4.4.1 The longitudinal variables

The variables generally used to describe the longitudinal particle motion, as a function of *s*, are:

- ϕ, the absolute particle phase, calculated from the RF frequency, with $\phi = 0$ arbitrarily chosen.
- *W*, the particle kinetic energy[7].

The evolution of these variables with *s* is given by the equations:

$$\begin{cases} \dfrac{d\phi}{ds} = \dfrac{\omega_{rf}}{\beta_z c} = \dfrac{2\pi}{\beta \cdot \lambda_{rf} \cdot \sqrt{1 - x'^2 - y'^2}} \\ \dfrac{dW}{ds} = q \cdot \left(x'E_x(s,\phi,r) + y'E_y(s,\phi,r) + E_z(s,\phi,r) \right) \end{cases} . \tag{48}$$

[7] This is really a 'longitudinal' particle property only in paraxial approximation.

Applying these equations to the synchronous particle, one gets:

$$\begin{cases} \dfrac{d\phi_s}{ds} = \dfrac{2\pi}{\beta_s \cdot \lambda_{rf}} \\ \dfrac{dW_s}{ds} = q \cdot E_z(s, \phi_s, 0) \end{cases} . \tag{49}$$

Let us define the reduced phase and energy variables for each particle:

$$\begin{cases} \varphi = \phi - \phi_s \\ w = W - W_s \end{cases} . \tag{50}$$

Late particles have a positive φ.

The equations of motion with these new variables become:

$$\begin{cases} \dfrac{d\varphi}{ds} = \dfrac{2\pi}{\lambda_{rf}} \cdot \left(\dfrac{1}{\beta \cdot \sqrt{1 - x'^2 - y'^2}} - \dfrac{1}{\beta_s} \right) \\ \dfrac{dw}{ds} = q \cdot \left[x' E_x(s, \phi, r) + y' E_y(s, \phi, r) + E_z(s, \phi, r) - E_z(s, \phi_s, 0) \right] \end{cases} \tag{51}$$

When the beam is accelerated by a standing-wave cavity structure, synchronous particles enter successive cavities giving it a strong energy gain, separated by long drift spaces where no acceleration occurs. In order to understand the physics, this periodic acceleration scheme can be replaced by a continuous acceleration one. This scheme assumes that the beam is accelerated by a travelling wave propagating at the same speed as that of the synchronous particle. This scheme allows a mathematical resolution of the dynamics equations[8] with an electric field independent of *s*.

4.4.2 The electric field model

The electric field, generally a function of *s*, is the chosen constant. The field amplitude of the travelling wave is E_0T (mean electric field) on axis. Here E_0 is defined as the potential gain of one cavity V_0 divided by the distance between the centres of consecutive cavities. The transit-time factor T has been included to take into account the variable efficiency of the acceleration in standing-wave cavities with the particle velocity.

The on-axis electric field longitudinal component becomes:

$$E_z(s, \varphi, r = 0) = E_0 T \cdot \cos(\varphi + \phi_{s0}), \tag{52}$$

ϕ_{s0} being the RF synchronous phase of the synchronous particle.

The energy gain per metre of the synchronous particle is then:

$$G = qE_0T_s \cdot \cos\phi_{s0}. \tag{53}$$

Here T_s is the transit-time factor of the synchronous particle.

Let us assume an *axisymmetric accelerating field*, the off-axis electric field longitudinal component can be written:

$$E_z(s, \phi, r) = E_0 T \cdot R(r) \cdot \cos(\varphi + \phi_{s0}), \tag{54}$$

[8] Equations are smoothed for analytic solutions, then quantified for a numerical solution.

r being the radial position of the particle, $R(r)$ expressing the radial evolution of the electric field longitudinal component. It can usually be written as $R(r) = 1 + O\left(r^2\right)$. Close to the axis, the Bessel function, solution of the Maxwell equations in axisymmetric geometry in vacuum, can be used to express $R(r)$ [2][6], but far from the axis, the cavity geometry has a strong influence through the boundary conditions. The radial position (r) can be replaced by (x,y) if the cavity is not axisymmetric. Some authors include the variation of the field with r in the transit time factor: $T(r)$.

From the relationship $\vec{\nabla} \cdot \vec{E} = 0$ and remarking that the electric field transverse component is null on the axis, one gets the electric field transverse component:

$$\begin{aligned} E_r\left(s, \varphi, r\right) &= -\frac{1}{r} \cdot \int_0^r \frac{\partial E_z\left(s, \varphi, r\right)}{\partial s} \cdot r \cdot dr \\ &= -\frac{1}{r} \cdot \frac{E_0 T}{\beta_s \lambda} \cdot \sin\left(\varphi + \phi_{s0}\right) \cdot \int_0^r R\left(r\right) \cdot r \cdot dr \quad . \end{aligned} \tag{55}$$

The electric field radial component can be written:

$$E_r\left(s, \varphi, r\right) = -\frac{E_0 T}{\beta_s \lambda} \cdot \sin\left(\varphi + \phi_{s0}\right) \cdot \left(\frac{r}{2} + O\left(r^3\right)\right) . \tag{56}$$

Three assumptions are made to decouple the longitudinal motion from the transverse one:

– In general, we assume:

$$\frac{r}{2} + O\left(r^3\right) << \beta_s \lambda \text{ . As } \left(x', y'\right) << 1 \quad ,$$

and the contribution of the transverse electric field to the energy gain can usually be neglected in Eq. (51):

$$x' E_x + y' E_y << E_z - E_{zs} . \tag{57}$$

– Generally, the *paraxial assumption* occurs, and we consider:

$$x'^2 + y'^2 << 1. \tag{58}$$

– Finally, we assume that the longitudinal field does not depend on the radial position r, by taking:

$$R(r) \approx 1. \tag{59}$$

4.4.3 The equations of motion

Using these assumptions, Eqs. (51) become:

$$\begin{cases} \dfrac{d\varphi}{ds} = -\dfrac{2\pi}{\lambda}\left(\dfrac{1}{\beta(s)} - \dfrac{1}{\beta_s(s)}\right), \\ \dfrac{dw}{ds} = -q \cdot E_0 T \cdot \left(\cos\phi_{s0} \cdot \left(1 - \cos\varphi\right) + \sin\phi_{s0} \cdot \sin\varphi\right) \quad , \end{cases} \tag{60}$$

which is in fact the equation of motion of on-axis particles.

Moreover, *a small longitudinal velocity dispersion* assumption can be carried out:

$$\frac{1}{\beta} - \frac{1}{\beta_s} = \delta\beta^{-1} << \frac{1}{\beta_s}, \tag{61}$$

and a *first order development* around synchronous velocity gives:

$$\delta\beta^{-1} = -\frac{w}{(\beta_s\gamma_s)^3 \cdot mc^2}.$$

If one considers that the transit-time factor does not depend on the beam particles' energy:

$$T(w) = T_s, \tag{62}$$

Eq. (60) becomes:

$$\begin{cases} \dfrac{d\varphi}{ds} = -2\pi \cdot \dfrac{w}{(\beta_s\gamma_s)^3 \cdot mc^2 \cdot \lambda} = \dfrac{\partial H_{\phi w}}{\partial w} \\ \dfrac{dw}{ds} = -q \cdot E_0 T_s \cdot \left[\cos\phi_{s0} \cdot (1-\cos\varphi) + \sin\phi_{s0} \cdot \sin\varphi\right] = -\dfrac{\partial H_{\phi w}}{\partial \varphi} \end{cases}. \tag{63}$$

As φ and w are canonical variables with the independent variable s, a Hamiltonian $H_{\varphi w}$ has been used to describe the particle motion:

$$H_{\varphi w} = -\frac{2\pi}{(\beta_s\gamma_s)^3 \cdot mc^2 \cdot \lambda} \cdot \frac{w^2}{2} - q \cdot E_0 T_s \cdot R(r) \cdot \left[\sin\phi_{s0} \cdot (\cos\varphi - 1) + \cos\phi_{s0} \cdot (\sin\varphi - \varphi)\right] \tag{64}$$

In the phase space (φ, w), particles follow curves where $H_{\phi w}$ = Cst. They are represented in Fig. 5 for on-axis particles. In Fig. 5(a), $\beta_s\gamma_s$ = Cst, as in Fig. 5(b), an adiabatic acceleration ($\beta_s\gamma_s \neq$ Cst) is added and the bucket turns into the well-known *golf club* shape.

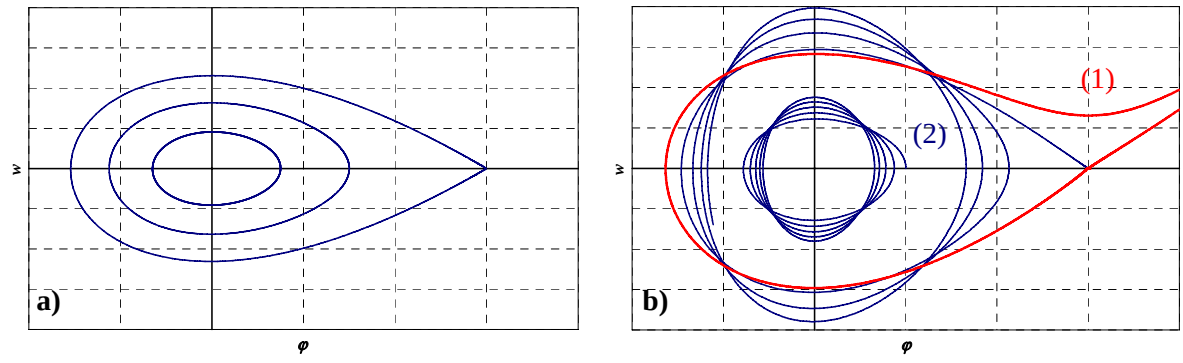

Fig. 5: Particle trajectories in longitudinal phase-space. (a) $\beta_s\gamma_s$ = Cst. (b) Adiabatic acceleration: the *golf club* represents the input acceptance [in red, (1)]. In blue (2) are the trajectories of two particles. They exhibit the damping of the phase oscillation amplitude with acceleration.

A particle entering the cavity after the synchronous particle gets a larger energy gain. A particle entering the cavity in advance (called the early particle) gets a smaller energy gain.

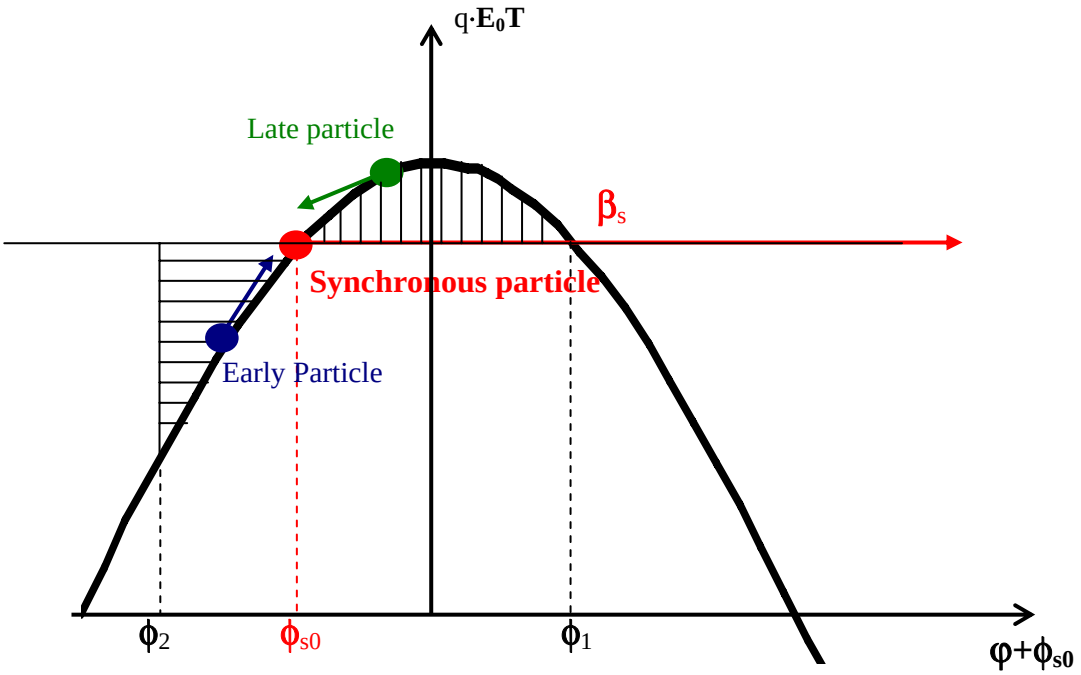

Fig. 6: Energy gain—synchronous particle

The synchronous phase of the synchronous particle is a stable point situated between –π/2 and 0 [9].

The choice of the synchronous phase delimits a phase acceptance:

– The higher limit ϕ_1 is the phase where a late particle gets the same energy gain as the synchronous particle:

$$\phi_1 = -\phi_{s0} \qquad \Rightarrow \qquad \varphi_1 = -2 \cdot \phi_{s0} \ . \tag{65}$$

– At the lower limit ϕ_2, the confinement potential equals the potential at the higher limit (ϕ_1). As the potential is the integral of the force, ϕ_2 is the phase where the horizontally hatched surface (in Fig. 6) equals the vertically hatched one. It can be calculated from the Hamiltonian given in Eq. (64):

$$H_{\varphi w}(\varphi = \phi_2 - \phi_{s0}, w = 0) = H_{\varphi w}(\varphi = \phi_1 - \phi_{s0}, w = 0). \tag{66}$$

ϕ_2 is the solution of

$$(\sin\phi_2 - \phi_2 \cos\phi_{s0}) + (\sin\phi_{s0} - \phi_{s0}\cos\phi_{s0}) = 0 . \tag{67}$$

– The choice of the synchronous phase also determines the energy acceptance ΔE corresponding to the difference between the potential energy of a particle with a phase ϕ_1 and the synchronous particle. It can also be calculated from the Hamiltonian given in Eq. (64):

$$H_{\varphi w}(\varphi = 0, w = \Delta E) = H_{\varphi w}(\varphi = \phi_1 - \phi_{s0}, w = 0) \ , \tag{68}$$

giving:

[9] For positively charged particles, as for negatively charged ones, it depends on convention (is $qE_0 > 0$ or $E_0 > 0$?).

$$\Delta E = 2 \cdot qE_0 T\left(\phi_{s0} \cos\phi_{s0} - \sin\phi_{s0}\right). \tag{69}$$

$$\Delta E = \left(\frac{\left(\beta_s \gamma_s\right)^3 \cdot \lambda \cdot mc^2}{\pi} \cdot 2 \cdot qE_0 T\left(\phi_{s0} \cos\phi_{s0} - \sin\phi_{s0}\right) \right)^{\frac{1}{2}}. \tag{70}$$

The acceptance area in the phase-energy space is called the *bucket*, its limit is called the *separatrix*. The energy acceptance ΔE and the phase ϕ_2 are represented as a function of the synchronous phase in Fig. 7.

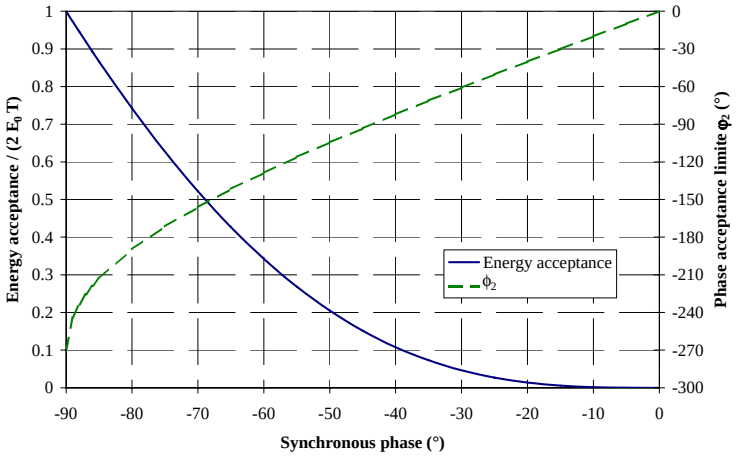

Fig. 7: Bucket dimensions as a function of the synchronous phase

For small phase amplitude oscillations, Eqs. (63) become:

$$\begin{cases} \dfrac{d\varphi}{ds} = -2\pi \cdot \dfrac{w}{\left(\beta_s \gamma_s\right)^3 \cdot mc^2 \cdot \lambda} \\ \dfrac{dw}{ds} = q \cdot E_0 T_s \cdot \sin\phi_{s0} \cdot \varphi \end{cases} \tag{71}$$

giving the second order differential equation of phase evolution:

$$\frac{d^2\varphi}{ds^2} + \frac{2}{\varsigma} \cdot \frac{d\varphi}{ds} + k_z^2 \cdot \varphi = 0 \tag{72}$$

with:

$$k_z^2 = \frac{2\pi q \cdot E_0 T_s \cdot \sin\left(-\phi_{s0}\right)}{\left(\beta_s \gamma_s\right)^3 \cdot mc^2 \cdot \lambda}. \tag{73}$$

Here k_z is the phase advance per metre of the beam core. In periodic structures of period L, $\sigma_z = k_z L$ is the longitudinal core phase advance per lattice.

$$\varsigma = \frac{2}{3} \cdot \frac{\beta_s \gamma_s}{d\left(\beta_s \gamma_s\right)/ds}. \tag{74}$$

Here ς is the damping length of the core oscillations.

Both ς and the variation of k_z with $\beta_s\gamma_s$ contribute to phase oscillation damping with acceleration. The adiabatic damping of the phase amplitude oscillation φ_a, defined when the contribution of ς is negligible, can be calculated [7]:

$$\varphi_a \propto \left(\beta_s \gamma_s\right)^{-3/4}. \tag{75}$$

Liouville's theorem implies that the energy amplitude oscillation w_a variation is

$$w_a \propto (\beta_s \gamma_s)^{3/4}.$$

The Hamiltonian in linear force then becomes:

$$H_{\varphi w} = -\frac{2\pi}{(\beta_s \gamma_s)^3 \cdot mc^2 \cdot \lambda} \cdot \frac{w^2}{2} + q \cdot E_0 T_s \cdot \sin\phi_{s0} \cdot \frac{\varphi^2}{2} \ . \tag{76}$$

The curves where the Hamiltonian is constant are then ellipses.

4.5 Motion in linear force

We have seen that the longitudinal particle motion is basically non-linear, but it can be linearized when the particle phase oscillation amplitude is very small compared to ϕ_1. The transverse forces are much more linear than the longitudinal ones, and the use of the linear focusing force is very close to reality, and can be solved analytically.

4.5.1 Linear transverse forces

In linacs, the main elements used to transport a beam are the cavities and the quadrupoles. Both these elements induce transverse forces.

4.5.1.1 Quadrupoles

In a perfect thick-lens quadrupole the magnetic field is

$$\begin{cases} B_x = G \cdot y \\ B_y = G \cdot x \end{cases} \tag{77}$$

where G is the quadrupole gradient (in T/m).

With the paraxial approximation and because the magnetic field does not change the particle's energy, the equations of transverse dynamics in quadrupole are then:

$$\begin{cases} \dfrac{d\gamma\beta_x}{ds} = \gamma\beta_z \dfrac{dx'}{ds} = -\dfrac{q \cdot G}{mc} x \\ \dfrac{dx}{ds} = x' = \dfrac{\beta_x}{\beta_z} \\ \dfrac{d\gamma\beta_y}{ds} = \gamma\beta_z \dfrac{dy'}{ds} = \dfrac{q \cdot G}{mc} y \\ \dfrac{dy'}{ds} = y' = \dfrac{\beta_y}{\beta_z} \end{cases} . \tag{78}$$

The transverse perfect quadrupole force is linear. Actually, fringe field and non-perfect hyperbolic poles induce non-linear effects which can generally be neglected at first order in linacs.

4.5.1.2 RF gap

When a particle travels through a cavity, the integration of the effect of the radial electric field and the azimuthal magnetic field can be modelized by a transverse kick, which is linear at second order. This kick modifies the particle transverse momentum:

$$\Delta(\gamma\beta_r) = -\frac{\pi q E_0 TL}{mc^2 \overline{\gamma\beta_z}^2 \lambda} \cdot \sin\phi \cdot \left[r + O\left(r^3\right) \right] = \Delta(\gamma\beta_z) \cdot r' + \gamma\beta_z \cdot \Delta r' \ , \tag{79}$$

with $\beta_r^2 = \beta_x^2 + \beta_y^2$. The term in r' shows that the particle transverse oscillation is damped by acceleration in accelerating cavities.

4.5.2 Motion of particle in periodic linear force

At first order, the motion of a particle can be linearized and the motion along all directions can be decoupled. The equation of motion in the *w* direction (*w* being *x*, *y* or φ) is the solution of a second-order equation:

$$\frac{d^2 w}{ds^2} + \frac{A_w}{\gamma\beta_z} \cdot \frac{d\gamma\beta_z}{ds} \cdot \frac{dw}{ds} + k_w(s) \cdot w = 0 . \tag{80}$$

Here A_w is a constant equal to 1 for $w = x$ or y, and 3 for $w = \varphi$.

Now, let us consider that the focusing force is periodic with period *S*, i.e. $k_x(s+S) = k_x(s)$. Generally, the damping term given by the acceleration is very small and can be considered as a perturbation:

$$\left\langle \frac{A_w}{\gamma\beta_z} \cdot \frac{d\gamma\beta_z}{ds} \cdot \frac{dw}{ds} \right\rangle_S << \left\langle k_w(s) \cdot w \right\rangle_S , \tag{81}$$

where $\langle a \rangle_S$ gives the average value of quantity *a* over one lattice period. In this assumption, the solution of Eq. (80) is:

$$w(s) = \sqrt{\beta_{wm}(s) \cdot I_w / \gamma\beta_z} \cdot \cos\left[\psi_w(s - s_0) + \psi_w(s_0)\right], \tag{82}$$

with β_{wm} periodic $\left[\beta_{wm}(s+S) = \beta_{wm}(s)\right]$, known as the structure beta function, solution of:

$$\frac{d^2\beta_{wm}}{ds^2} + 2 \cdot k_w(s) \cdot \beta_{wm} - \frac{2}{\beta_{wm}} \cdot \left[1 + \frac{1}{4} \cdot \left(\frac{d\beta_{wm}}{dt}\right)^2\right], \tag{83}$$

with $I_w / \gamma\beta_z$, known as the *Courant–Snyder* invariant (which is actually invariant with no acceleration), and ψ_w the particle phase advance, defined as:

$$\psi_w(s) = \int_{s_0}^{s} \frac{ds}{\beta_{wm}(s)} . \tag{84}$$

Particles are turning around periodic ellipses whose equations are:

$$\gamma_{wm}(s) \cdot w^2 + 2 \cdot \alpha_{wm}(s) \cdot w \cdot w' + \beta_{wm}(s) \cdot w'^2 = I_w / \gamma\beta_z , \tag{85}$$

with
$$\alpha_{wm}(s) = -\frac{1}{2} \frac{d\beta_{wm}(s)}{ds} , \tag{86}$$

and
$$\gamma_{wm}(s) = \frac{1 + \left[\alpha_{wm}(s)\right]^2}{\beta_{wm}(s)} . \tag{87}$$

The surface of the ellipses decreases as $1/\gamma\beta_z$ which is close to $1/\gamma\beta$ with the paraxial approximation.

The *phase advance per lattice* σ_w defined as

$$\sigma_w = \psi_w(s+S) - \psi_w(s), \tag{88}$$

gives an idea of how fast the particles turn around the ellipses. The number $2\pi/\sigma_w$ is the number of lattice periods when the particle has made one turn around the ellipses. One can note that, in linear forces, the phase advance per lattice is the same whatever the particle amplitude.

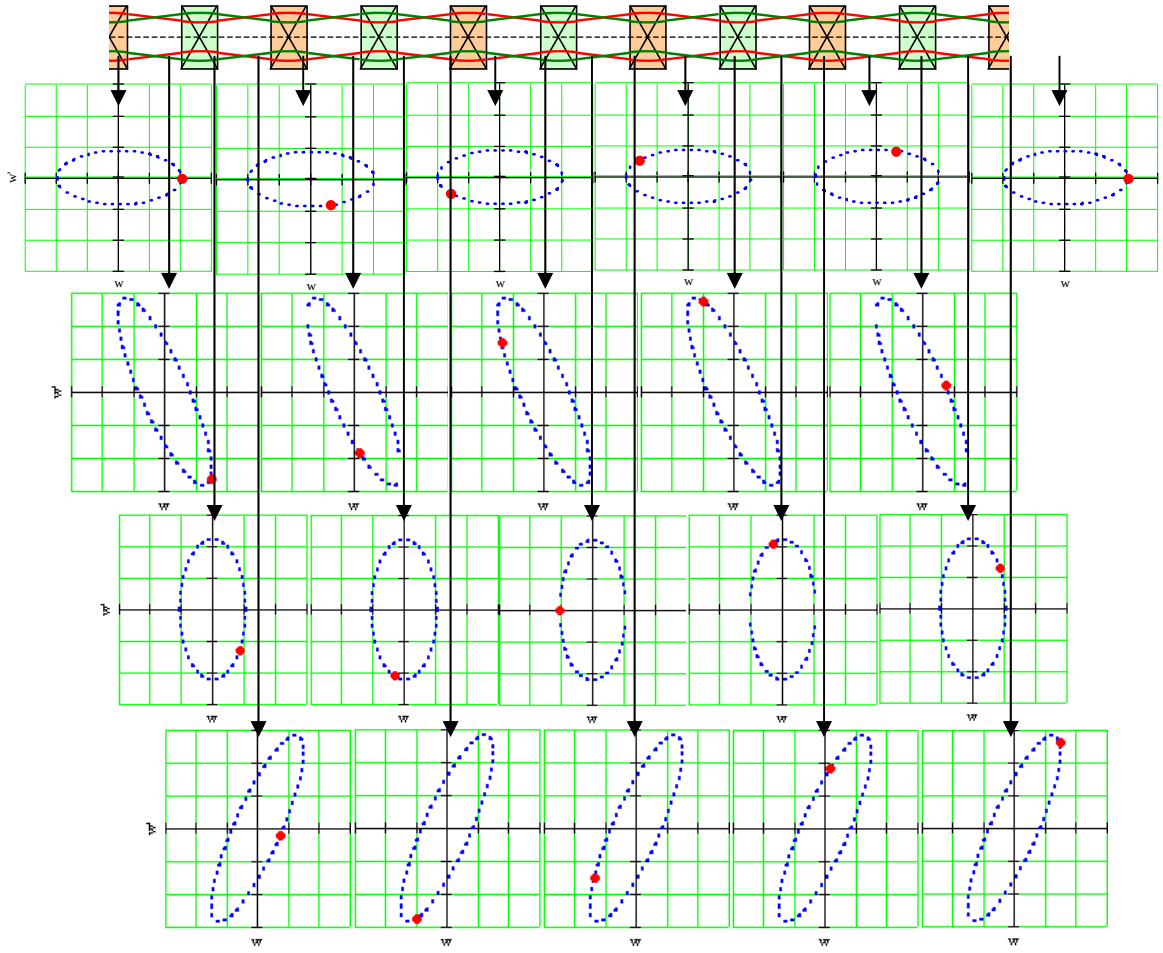

Fig. 8: Particle transport in a FODO channel

As an example, have a look at a particle motion along one direction in a FODO channel. In Fig. 8, five FODO lattices have been represented. The particle phase advance per lattice is 360°/5 = 72°. The particle position in 2D phase-space is represented by the red point in four different positions in the lattice. Each line correspond to one position:

– 1st line: middle of focusing quadrupole,

– 2nd line: between focusing and defocusing quadrupoles,

– 3rd line: middle of defocusing quadrupole,

– 4th line: between defocusing and focusing quadrupoles.

One observes that lattice after lattice the particle turns around an ellipse at the same position. The ellipse is different from position to position within the lattice. Its equation is given by (85). It is very important to understand that these ellipses have nothing to do with the beam (no beam has been defined here, just one particle). These ellipses are defined by the transport channel.

To conclude, we should keep in mind that a large number of assumptions have been made to achieve the results. The opportunity of each assumption has to be studied very carefully in practical cases. Nevertheless, the results presented here help to elucidate beam dynamics.

4.6 Beam r.m.s. dimension and Twiss parameters

A bunch is constituted of *N* particles. Its dimensions are defined statistically as follows:

– The beam centre of gravity position: $\langle w \rangle = \frac{1}{N} \sum_{i=1,N} w_i$. (89)

– The beam centre of gravity slope: $\langle w' \rangle = \frac{1}{N} \sum_{i=1,N} w'_i$. (90)

– The beam r.m.s. size: $\tilde{w} = \sqrt{\left\langle \left(w - \langle w \rangle \right)^2 \right\rangle} = \sqrt{\frac{1}{N} \sum_{i=1,N} \left(w_i - \langle w \rangle \right)^2}$. (91)

– The beam r.m.s. divergence: $\tilde{w}' = \sqrt{\left\langle \left(w' - \langle w' \rangle \right)^2 \right\rangle} = \sqrt{\frac{1}{N} \sum_{i=1,N} \left(w'_i - \langle w' \rangle \right)^2}$. (92)

– The beam r.m.s. emittance: $\tilde{\varepsilon}_w = \sqrt{\tilde{w}^2 \tilde{w}'^2 - \left\langle \left(w - \langle w \rangle \right) \cdot \left(w' - \langle w' \rangle \right) \right\rangle^2}$. (93)

The beam *Twiss parameters* are then deduced from the beam r.m.s. dimensions:

$$\tilde{\beta}_w = \frac{\tilde{w}^2}{\tilde{\varepsilon}_w}, \qquad \tilde{\gamma}_w = \frac{\tilde{w}'^2}{\tilde{\varepsilon}_w}, \qquad \tilde{\alpha}_w = -\frac{\left\langle \left(w - \langle w \rangle \right) \cdot \left(w' - \langle w' \rangle \right) \right\rangle}{\tilde{\varepsilon}_w}. \tag{94}$$

Generally, at least 90% of the particles in the bunch occupy an ellipse of equation[10]:

$$\tilde{\gamma}_w \cdot w^2 + 2 \cdot \tilde{\alpha}_w \cdot w \cdot w' + \tilde{\beta}_w \cdot w'^2 = 5 \cdot \tilde{\varepsilon}_w . \tag{95}$$

The parameter *w* can be *x*, *y*, *z* or φ. The phase-space 2D projections of a beam with ~100 000 particles are represented in Fig. 9. Ellipses in red correspond to ellipses calculated with Eq. (95). They contain, in this example, 92% of the particles.

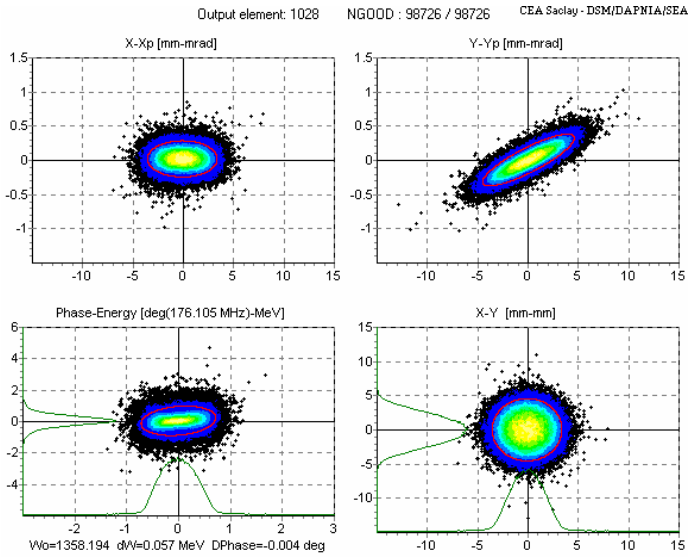

Fig. 9: Phase-space beam distribution and Twiss parameters

4.7 Matched/mismatched beam

A beam is matched when its Twiss parameters at a given position *s* correspond to the transport channel periodic Courant–Snyder parameters. In this condition, the same beam phase-space shape is

[10] If the bunch were uniform, 100% of the particles would occupy this ellipse.

reproduced period after period. The envelope evolution with *s* is periodic and as smooth as possible. In Fig. 10 the evolution of beams in the same FODO channel as before (upper line) has been represented. In the middle line, the ellipses represent the beams in the phase-space at the focusing quadrupole centre. The dashed-black circle represents a particle motion in this channel. One matched (in continuous red) and two mismatched (in dashed pink and dotted blue) beams have been represented. One particle of each beam has also been represented.

The matched beam ellipse is periodic, as one particle is replaced by another one. Its envelope (last line) is periodic with the lattice period *L*.

The mismatched beam ellipses sweep a bigger area (dashed-black circle) than the beam ellipse surfaces. Their envelope period is greater than the lattice period. Its oscillation is a combination of two oscillations with two different periods: one is the lattice period *L*, the other is $2\pi/\sigma_w \cdot L$, with σ_w being the channel phase advance per lattice.

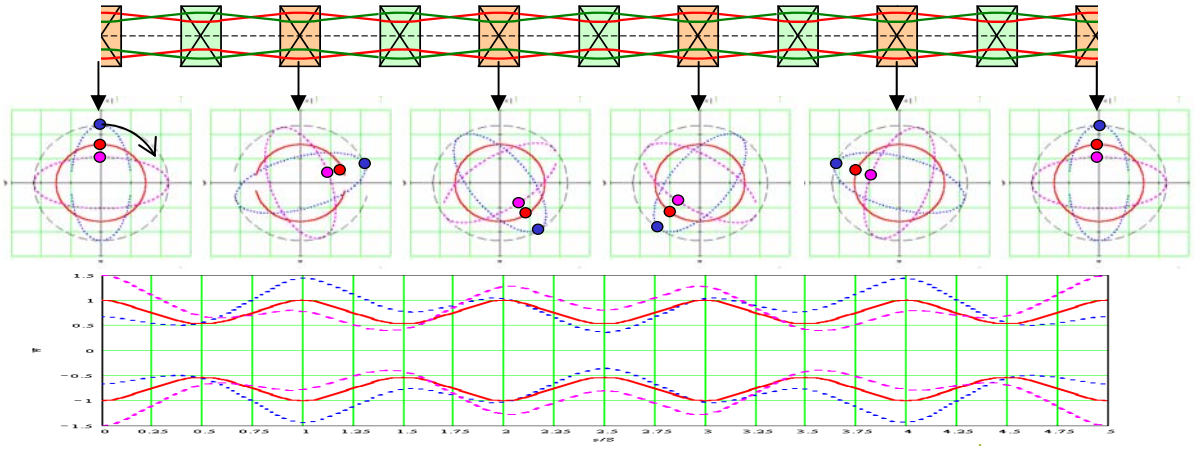

Fig. 10: Matched and mismatched beam in the FODO channel

When the *force is linear* (Fig. 11), all particles turn in the phase-space with the same period (i.e. the same phase advance per lattice). The beam phase-space distribution changes lattice after lattice, but its emittance is kept constant.

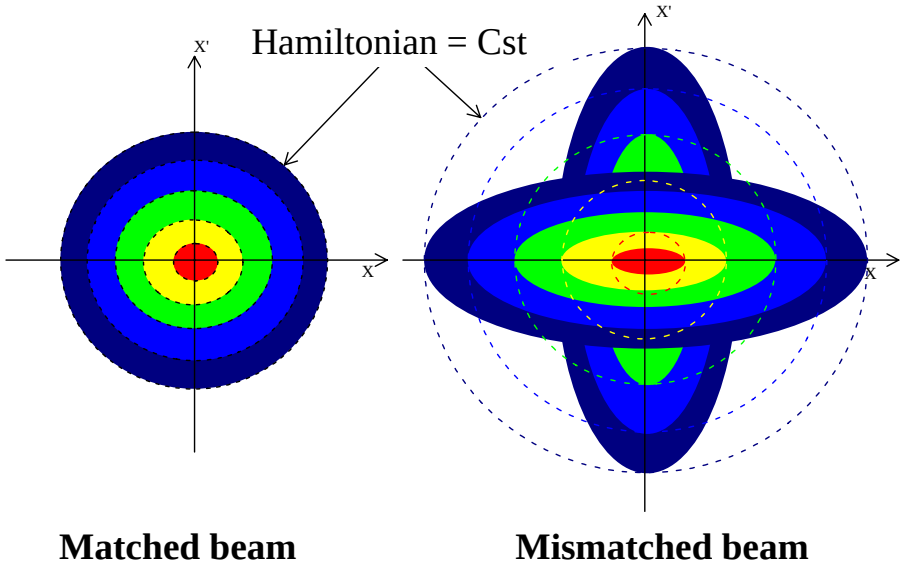

Fig. 11: Matched (left) and mismatched (right) beam in linear forces

When the *force is non-linear* (Fig. 12) [external force or force induced by space-charge (Coulomb interactions between beam particles)], the particle phase-advance per lattice depends on its oscillation amplitude. Beam particles no longer turn all at the same speed, and an apparent emittance growth is observed[11]. This effect is known as beam filamentation (Fig. 13). After a long time (many particle betatron periods), the phase-space swept by the beam is completely full of particles. The apparent emittance is higher.

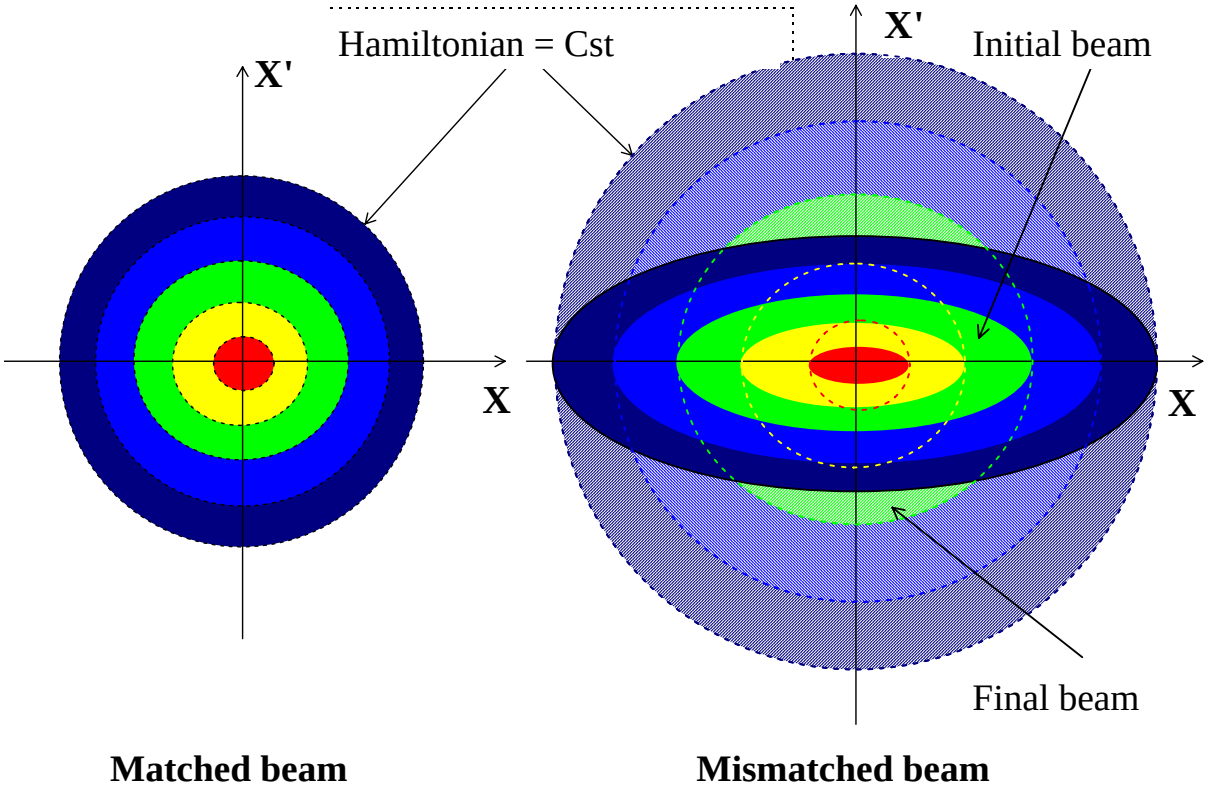

Fig. 12: Matched (left) and mismatched (right) beam in non-linear forces

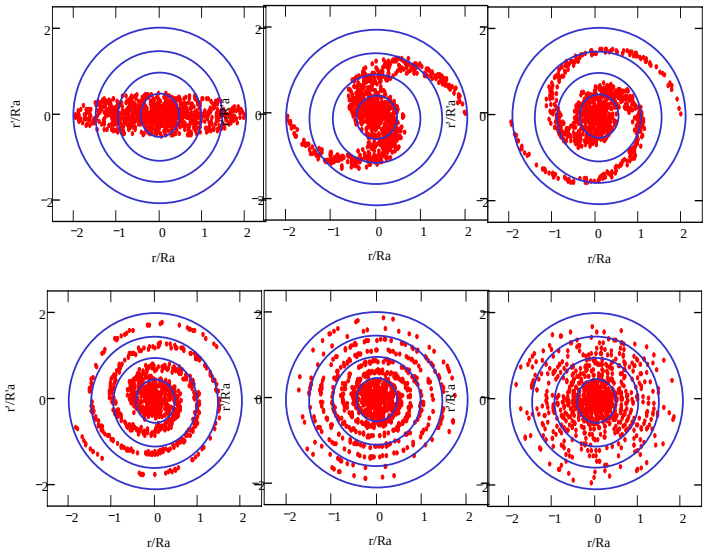

Fig. 13: Filamentation of mismatched beam in non-linear force

[11] Even if the phase-space area occupied by the particle is constant (Liouville's theorem applies).

5 CONCLUSION

This paper is a short introduction with basic notions on linacs. A better understanding cannot be obtained without tackling subjects like the existing structures, the RF control, the space-charge effects, or the resonances. Motivated students are strongly advised to read Tom Wangler's book [2].

ACKNOWLEDGEMENTS

Many thanks to Tom Wangler for his wonderful and very useful book on linacs, his encouragement and to my colleagues Romuald Duperrier and Didier Uriot for their help.

REFERENCES

[1] P.M. Lapostolle and A.L. Septier, *Linear Accelerators* (North-Holland, Amsterdam, 1970).

[2] T.P. Wangler, *Principles of RF Linear Accelerators* (Wiley, New York, 1998).

[3] CAS: CERN Accelerator School: *RF Engineering for Particle Accelerators*, Oxford, UK, 1991, Ed. S. Turner, CERN-92-03 (1992).

[4] T. Nishikawa, Transients and beam loading effect, in *Linear Accelerators*, Eds. P.M. Lapostolle and A.L. Septier (North-Holland, Amsterdam, 1970).

[5] M. Weiss, Introduction to RF linear accelerators, CAS: CERN Accelerator School: 5th General Accelerator Physics Course, Jyväskylä, Finland, 1992, Ed. S. Turner, CERN-94-01 (1994).

[6] A. Carne *et al.*, Numericals methods. Acceleration by a gap, in *Linear Accelerators*, Eds. P.M. Lapostolle and A.L. Septier (North-Holland, Amsterdam, 1970).

[7] J. Le Duff, Dynamics and acceleration in linear structures, CAS: CERN Accelerator School: 5th General Accelerator Physics Course, Jyväskylä, Finland, 1992, Ed. S. Turner, CERN-94-01 (1994).